



HAL
open science

Variety, growing conditions and processing method act on different structural and biochemical traits to modify viscosity in tomato puree

Miarka Sinkora, Anne-Laure Fanciullino, Nadia Bertin, Robert Giovinazzo, François Zuber, Alexandre Leca, Agnès Rolland-Sabaté, David Page

► To cite this version:

Miarka Sinkora, Anne-Laure Fanciullino, Nadia Bertin, Robert Giovinazzo, François Zuber, et al.. Variety, growing conditions and processing method act on different structural and biochemical traits to modify viscosity in tomato puree. Food Research International, 2024, 189, pp.114495. 10.1016/j.foodres.2024.114495 . hal-04617887

HAL Id: hal-04617887

<https://hal.inrae.fr/hal-04617887v1>

Submitted on 19 Jun 2024

HAL is a multi-disciplinary open access archive for the deposit and dissemination of scientific research documents, whether they are published or not. The documents may come from teaching and research institutions in France or abroad, or from public or private research centers.

L'archive ouverte pluridisciplinaire **HAL**, est destinée au dépôt et à la diffusion de documents scientifiques de niveau recherche, publiés ou non, émanant des établissements d'enseignement et de recherche français ou étrangers, des laboratoires publics ou privés.



Distributed under a Creative Commons Attribution - NonCommercial 4.0 International License



Variety, growing conditions and processing method act on different structural and biochemical traits to modify viscosity in tomato puree

Miarka Sinkora^a, Anne-Laure Fanciullino^{b,c}, Nadia Bertin^c, Robert Giovinazzo^d, François Zuber^e, Alexandre Leca^a, Agnès Rolland-Sabaté^a, David Page^{a,*}

^a INRAE, Avignon Université, UMR SQPOV, F-84000 Avignon, France

^b INRAE, PSH, F-84000 Avignon, France

^c Univ Angers, Institut Agro, INRAE, IRHS, SFR QUASAV, F-49000 Angers, France

^d Société Nationale Interprofessionnelle de la Tomate, Avignon, France

^e ZA Aeroport, CTCPA Ctr Tech Conservat Prod Agr, F-84911 Avignon 9, France

ARTICLE INFO

Keywords:

Tomato puree
Break process
Rheology
Pectin
Particles
Puree structure

ABSTRACT

The texture of tomato products can be modified by choice of variety, their growing conditions and/or processing method, but no clear explanation exists of the mechanisms that transform fruit tissue, how they act on texture, or whether genetics and processing impact the same physical parameters. We therefore conducted a study that processed 4 varieties produced under low/high nitrogen supply, into puree using both hot and cold break processes. No specific rheological signature allows discrimination between cultivar-induced or process-induced textural changes, but that they can be distinguished by sensory analysis. Growth conditions impacted but was not sensory distinguished. Both caused significant variations in 7 of 11 physico-chemical parameters, but the order of importance of these traits controlling texture varied, depending on whether the cause was genetic or process-related. Analysis of alcohol insoluble solids revealed a specific signature in pectin composition and conformation that could be linked to particle aggregation in the presence of lycopene-rich particles.

1. Introduction

Processed tomatoes are food base products and tomato paste heads the list of processed products. In 2021, production worldwide totalled 38.7 million metric tonnes, from major producers such as California (10.7 M mT), Italy (6.05 M mT) and China (4.8 M mT) and smaller players such as France (164 000 mT) (WPTC, 2021). Growing awareness of climate change and anthropogenic pollution prompts growers to adopt more sustainable practices which in turn impact the quality of harvested fruit (Vilas Boas et al., 2017). As a result, tomato processors must adapt their practices to maintain the quality of the finished product. The quality attributes of puree, in order of importance for the consumer, are texture, colour and flavour (Hayes et al., 1998). Such is the importance of texture that it is of interest even to the engineering industry, where it is used to define appropriate parameters and influences the design of machinery such as pumps (Rao, 2014). For the most part, no texture agents are added to the tomato puree. Consequently, the desired texture must be obtained by use of appropriate processing parameters adjusted for the specific quality of a fruit.

Varieties have long been selected for traits associated with the quality of the processed product. Despite the use of breeding to improve yields since the 1930s, the complexities of viscosity improvement have yet to be untangled (Ronga et al., 2019).

Purees are suspensions of insoluble particles (pulp) in a continuous phase (serum). Their respective proportions, compositions and interactions impact their rheological properties. Particles are mainly individual cells and cell fragments (Lopez-Sanchez et al., 2011), but may also result from the aggregation of smaller elements (Bayod et al., 2007). Their distribution is bimodal, with one class of particles larger than 100 μm , and another where particles are about 1 μm in size (Bayod & Tornberg, 2011). Tomato products behave like weak gels, with dominant elastic properties. Their storage modulus (G') is systematically higher than their loss modulus (G'') in the linear viscoelastic domain. From a physical point of view, tomato purees are pseudoplastic fluids with a yield stress, and their flow behaviour above the yield stress fits well with a power law equation (Diantom et al., 2017; Koocheki et al., 2009; Lee et al., 2002).

Texture can be modified by either the processing method or choice of

* Corresponding author.

E-mail address: david.page@inrae.fr (D. Page).

<https://doi.org/10.1016/j.foodres.2024.114495>

Received 11 January 2024; Received in revised form 30 April 2024; Accepted 7 May 2024

Available online 8 May 2024

0963-9969/© 2024 The Authors. Published by Elsevier Ltd. This is an open access article under the CC BY-NC license (<http://creativecommons.org/licenses/by-nc/4.0/>).

variety. Processing can be either cold break (CB) or hot break (HB). CB consists in chopping tomatoes and maintaining their temperature at 60 to 66 °C for a short period to allow the pectinolytic enzymes to react, before stabilizing the product at around 95 °C, while for HB, chopping is performed at 93 to 99 °C, immediately inactivating enzymes (Barringer, 2004). Consequently, HB products are more viscous and darker, while CB products are more liquid and redder, with flavours closer to the fresh fruit (Goodman et al., 2002). With regard to genetics, to our knowledge, texture has never been directly addressed as a breeding trait in its own right, having been addressed only indirectly through the improvement of fruit dry matter content or soluble solid content. In the latter case, though, it was recorded that there was no link to texture variation (Vilas Boas et al., 2017). The complexity of the mechanisms underlying texture modification in purees has been partially documented (Sánchez et al., 2002), but we still lack basic knowledge to define breeding traits more precisely, and if they are influence by cropping conditions.

More is known on the effects of processing methods. HB processing and a longer concentration step (i.e. higher soluble solid content) both increase apparent viscosity, yield stress, and storage and loss moduli (Porretta, 2019). HB/CB impact the cell wall, which is composed of cellulose, hemicelluloses and pectins. These last accumulate in the middle lamella and act as linkers between cells. They are therefore key components of fruit texture. Their properties vary according to their constitutive monosaccharides, their degree of polymerisation, their linear or branched structure, and the degree of methylation (DM) of their galacturonic acid units (BeMiller, 2018), thus modifying the puree texture. The DM may have contrasting effects as it can either increase gelling properties (in contexts of high DM where the sucrose content and pH are high and it depends on hydrophilic bonds), or decrease them (in low DM, low-sugar and high-calcium contexts, by favouring ionic bonds). These variations make it difficult to predict its impact on texture (Gawkowska et al., 2018). During CB processing, pectinolytic enzymes catalyze their degradation. Pectinmethylesterase (PME) catalyses the demethoxylation of the homogalacturonan acid units, allowing their hydrolysis by the polygalacturonase (PG), leading to a decrease of viscosity (Sánchez et al., 2002). A high break temperature such as that in HB processing inactivates enzymes at an early stage of processing, leading to higher viscosity, yield stress and viscoelastic moduli, due to a higher water-insoluble solid content (Valencia et al., 2004). High-performance size-exclusion chromatography coupled with multi-angle-laser-light scattering (HPSEC-MALLS) on serum has shown that the root-mean-square (rms) radius of pectins decreased during puree concentration while the molar mass remained constant, leading to a loss of viscous properties (Diaz et al., 2009). Processing method may also impact particle size distribution, although there are discrepancies in the reported effects of particle size, shape, concentration and deformability on rheological behaviour (Porretta, 2019). On the one hand, viscosity is reported to increase when the proportion of small particles is increased either after the reconstitution of purees following wet sieving (Yoo & Rao, 1994) or by performing additional homogenisation operations (Bayod et al., 2007). Elsewhere, though, studies reported optimum viscosity in particles measuring between 90 and 180 µm, with a decrease in viscosity for larger particles (Ouden & Vliet, 2006), and no modification of the storage modulus after particle size was decreased by homogenisation (Moelants et al., 2014). Not only the size, but also the shape of particles modifies their rheological properties. Irregular particle surfaces increase yield stress (Leverrier et al., 2017; Moelants et al., 2014). A better understanding of the respective roles of serum viscosity and particle shapes and sizes must be achieved in order to set quality targets.

Thirty-three sensory attributes have been proposed by trained panels to describe fresh and processed tomatoes, comprising aroma, texture, flavour, basic taste and mouthfeel attributes. Three of them concern texture of purees (pulp amount, thickness and viscosity) (Hongsongnern & Chambers, 2008), and are assessed visually (e.g., visible mealiness), with spoon tests (stirring or pouring) or in-mouth by

chewing the product. However, given that sensory texture is a highly connected set of attributes, instrumental analysis struggles to evaluate overall sensory texture. Any instrumental measurement of texture should therefore be corroborated at least by a hedonic test to verify that the differences measured are really perceived by the consumer. The napping method is a non-directed method designed to distinguish wines taking multiple attributes into account (Pages et al., 2015) and can be adapted to assess rheological measurements on tomatoes.

Against this background, the present study aimed to i) analyse the variations in the rheological properties of tomato puree induced by interactions between break process, cultivar and nitrogen supply (as an example of contrasted growing conditions), ii) assess whether measured differences were perceived by consumers, and iii) relate viscosity changes to structural and biochemical characteristics and identify which of these explain the effects of processing and variety. The starting hypothesis was that the textural changes induced by contrasted processing methods or cultivar selections stem from different rheological parameters and that a detailed analysis of these parameters will help improve the quality of end products by enabling the break process to be matched to the raw material and the breeding of new varieties suited to current and future contexts of production.

2. Material and methods

2.1. Plant material and fruit harvesting

Four varieties (H1311, Terradou, Lykopol and Sailor) were cultivated in 2019 and 2020 in an open field near Avignon, France (44°11'22.4"N 4°48'11.7"E). Varieties were randomly distributed in the field in order to obtain double rows of 50 to 100 m in length at a linear density of 3.3 plants per meter. Plants were drip irrigated and irrigation was adjusted weekly based on climate data from a local weather station to replace 100 % of the plant evapotranspiration (Vilas Boas et al., 2017). In 2019, the experimental design consisted in two varieties (Terradou and H1311) cultivated under two contrasting levels of nitrogen supply (high = 73 kg/ha, low = 21 kg/ha). In 2020, four varieties (H1311, Terradou, Lykopol and Sailor) were cultivated in another field located very close to the first under high nitrogen supply (100 kg/ha). Thus, a total of 8 different batches of 200 kg, corresponding to the 8 combinations (2 varieties and 2 N levels in 2019 and 4 varieties in 2020) were harvested for processing. Red fruits were selected (representing 71 and 90 % of the total fruit mass per plant in 2019 and 2020 respectively). During the harvest, three 2 kg-aliquots of fruits were collected on plant from three locations along each plots of the 8 combinations and were stored as fresh representative fruits. Therefore. A central slice (about 1 cm thick) were cut into each fruits of the aliquots. The slices of each aliquot were diced altogether, quickly frozen and stored at -80 °C until analysis.

2.2. Processing

Each of the 8 batches were separated in two parts and each part were processed using either "hot-break" (HB) or "cold-break" (CB) methods, in a pilot plant (CTCPA, Avignon, France), giving a total of 16 purees. Processes were adapted from Barrett et al. (1998) as follow. For CB juices, the tomatoes were cleaned, chopped in a hammer mill (Electra F6N, Electra, France), heated for 3 min at 50 °C in a scraped-surface heat exchanger (Thermorotor, Duprat, France) and directly refined. Under the HB method, juices were extracted and refined at ambient temperature in a turbo extractor equipped with an 8/10 sieve (Giubillo short 55KW, CFT, Italy), vacuum deaerated and immediately heated for 2 min at 95 °C under ohmic heating (Ohmico impianto pilota, CFT, Italy), chambered for 5 additional minutes at 95 °C in a vapor exchanger, and then homogenized and cooled to 40 °C in a tank. The HB and CB juices were then concentrated to approximately 15 °Brix in a vacuum evaporator at 55 °C (Auriol, France). Concentrates were canned,

sterilized for 25 min at 93.3 °C ($z = 8.89$ °C) in a vertical static autoclave (AUTR03, Auriol, France) and the cans were then stored at 4 °C until analysis.

2.3. Sensorial analysis (napping)

Purees were tasted in 2019 and 2020 by 14 untrained panels using the napping method (Pagès, 2005). The purees were transferred into 50 ml cups before tasting, and their order of presentation was randomized for each panel. The tasting cups were placed by the panel members on a paper tablecloth (60x40), according to their similarities or differences. Sample positions were characterized by coordinates on the tablecloth and the coordinates were analyzed using multiple factor analysis to produce an average map of individuals showing the average position of samples and their confidence ellipses (Pagès & Husson, 2005). Data analysis was conducted with the FactoMineR R package.

2.4. Rheological measurements

Rotational and oscillatory tests were conducted as described in (Buergy et al., 2020) with a few adaptations to tomato purees. All tests were performed on a stress-controlled rheometer (Physica MCR301, Anton Paar, Austria) equipped with a Peltier cell (CPTD -200, Anton Paar). Samples were thermostated at 22.5 °C and changed for each test. Tests were performed with a six-bladed vane tool (FL 100/6W/Q1, Anton Paar) within an outer cylinder cup (CC27/S, Anton Paar). A third test using a double helicoidal ribbon mobile (ST24-2HR-37/120, Anton Paar) within the same outer cylinder was performed in order to verify that the shear rate was not influenced by the wall slip phenomenon known to occur in tomato products (Moelants et al., 2013). Each test was preceded by a pre-shearing at 20 s^{-1} during 60 s, and a 300 s rest with the mobile remaining in the product, to remove trapped air, ensure the product was dispersed and allow it to regain rheological equilibrium. Three tests were performed for each puree:

1- a flow curve consisting of apparent viscosity measurements over a range of shear rates from 1 to 150 s^{-1} (31 points automatically scaled over a logarithmic ramp) following 15 s of stabilization for each point. The flow curves were then modelled using the Ostwald de Waele equation (Equation 1) suitable for non-Newtonian fluids (Kubo et al., 2019).

$$\eta = K \times \dot{\gamma}^{(n-1)}$$

Equation 1: Ostwald de Waele's modelling of viscosity as a function of shear rate, where η is the apparent viscosity in Pa.s, K is the consistency coefficient in Pa.s^n , $\dot{\gamma}$ is the shear rate in s^{-1} and n is the flow behaviour index (dimensionless).

2- an oscillatory strain sweep was performed to define the linear viscoelastic domain (constant G' and G''). Strain was applied from 0.01 to 150 % (logarithmic ramp) at a frequency of 1 Hz and 20 points were registered for both the loss modulus (G'') and the storage modulus (G'). The flow stress (FS) was estimated from the curves as the point where G' and G'' equalized as both left the linear domain (Buergy et al., 2020). A frequency sweep was then performed within the previously defined linear viscoelastic domain. Here, oscillatory shear was applied under a constant strain of 1 %, but with frequencies varying from 0.01 to 100 Hz, giving access to more accurate measurements for G' and G'' . Loss factor $\tan(\delta)$ was then calculated as the ratio of the storage modulus G' to the loss modulus G'' . The phase shift δ was calculated as the arctangent of the loss factor.

3- Apparent viscosity η_{50} was measured with a double helicoidal ribbon mobile at a shear rate of 50 s^{-1} to mimic the shearing applied by in-mouth puree consumption (Stokes, 2012).

Serum viscosity (obtained by centrifugation, described below) double gap geometry measuring system (DG27 + DG27/T200/SS, Anton Paar, inner gap = 0.982 mm, outer gap = 1.136 mm). After a 60 s rest, a

flow curve from 10 to 1000 s^{-1} was produced (logarithmic ramp), from which the apparent viscosity value of 100 s^{-1} was selected as being representative of the shear rate applied during in-mouth serum consumption (Buergy et al., 2020).

2.5. Pulp to serum distribution

The pulp to serum distribution was calculated according to Espinosa-Munoz et al. (2013) with a few adaptations for tomato products: three replicates of 12 g of each puree were centrifuged in 12 mL tubes on a Beckman ultracentrifuge (L8-70 M, Beckman, USA) equipped with a swing rotor (SW41T, average diameter 61,2mm) at 100,000 g, at 4 °C, for 28 min (including 4 min of acceleration). The pulp volume fraction was calculated as the ratio between the pellet volume and the total volume in the tube (supernatant + pellet). The serum was then removed for further rheological analysis, and the pulp was weighed and analysed for dry matter content (DMC). The pulp DMC fraction was calculated as a proportion of the total puree on a dry-weight basis.

2.6. Particle-size distribution of insoluble fraction and microscopy

Wet sieving of 80 g of puree was performed on a vibratory sieve shaker (Retsch AS200 Basic, Retsch, Germany) with an 80 μm -mesh sieve (Page et al., 2019). Samples were washed with 1 L to 1.5 L of distilled water until the rinsing water became clear. Particles retained on the sieve, hereafter called "large particles" (LP) were centrifuged (9000 g for 10 min), as were those contained in the rinsing water (9000 g for 20 min) hereafter called, "small particles" (SP). The pellets in both sieving fractions were weighed and analysed for dry matter content and their particle size distribution was analysed using a laser diffraction analyser (Mastersizer 2000, Malvern Instruments Ltd, UK). Samples were dispersed in distilled water (refractive index 1.33). The refractive index of the particles was set at 1.52 and absorption at 0.1 (Leverrier et al., 2016). Each sample was analysed in triplicate, and for each analysis, an average particle size calculated from three measurements was considered.

SP observation was prepared according to Lan et al. (2020), with few modifications: 2 mg of SP were diluted in 2 mL of distilled water containing 0.01 % of calcofluor and were observed under a microscope (Olympus BX61, Olympus, Japan) with x20 magnification. One drop of diluted pellet was placed on a 1 mm pre-cleaned micro slice (Leica biosystems, Germany) covered by glass 0.16–0.19 mm thick. For each sample, three slides were studied and 10 images were recorded per slide. A total of 103 images were analysed. In each image, particles longer than 20 μm were counted and measured under FITC (lycopene autofluorescence) and DAPI (cell wall material coloured with calcofluor). The DAPI and FITC images were merged to verify the colocation of the lycopene particles and the cell wall material.

2.7. Biochemical traits

All biochemical analysis was conducted in triplicate on fresh tomato ground under liquid nitrogen using an IKA A11 basic analytical mill (IKA Works, USA) and on purees. The dry matter content (DMC) was determined by weighing 3 g of fresh sample before and after 3 days of drying at 70 °C, total soluble solid content (TSS) was measured with a refractometer (ATAGO PR-32 α , Japan), pH was measured with a pH meter (Mettler Toledo, Switzerland) inserted directly into the purees. Titratable acidity (TA) was measured with an automatic 888 Titrand titrator (Metrohm, Switzerland), and results were expressed in $\text{mEq } 100 \text{ g}^{-1}$ fresh weight using the Tiamo 2.4 software.

Enzymatic activities were measured on the same freeze-ground powder. PG activity was determined by the Gross method adapted by (Ribas-Agustí et al., 2017). PME activity was determined by an adaptation of the HOUBEN method described by (Ribas-Agustí et al., 2017). The PME enzyme extract aliquot was 50 μL rather than 250 μL due to the

high enzyme activity in tomato fruit.

Alcohol insoluble solids (AIS) were extracted from 2 g of freeze-ground powder or from 2 g of freeze-dried purees as described in (Le Bourvellec et al., 2011). Samples were previously stirred for one night at 4 °C in pure acetone to remove carotenoids. AIS were expressed as a percentage of initial dry weight.

Neutral sugars, galacturonic acid (GalA) and methanol were measured in AIS following acid hydrolysis (Saeman et al., 1954). Free neutral sugars were derivatized to alditol acetates (Englyst et al., 1982) and analysed by gas chromatography, GalA was measured by spectrophotometry using the *m*-hydroxydiphenyl assay (Blumenkrantz & Asboe-Hansen, 1973), and methanol was quantified using stable isotope dilution (Buergy et al., 2020). The degree of methylation (DM) was evaluated as the molar ratio between methanol and GalA. Pectin composition was assessed by means of four neutral sugar quantity ratios (in mg/g): GalA divided by the sum of rhamnose, arabinose and galactose to assess the level of branching (R1); the sum of arabinose and galactose divided by rhamnose to assess the length of branching chains (R2); GalA divided by rhamnose to assess pectin linearity (R3); and arabinose divided by galactose to assess the type of branching (R4).

The molar mass and size distributions of soluble pectin were evaluated on a high-performance size-exclusion chromatograph (HPSEC) connected to a multi-angle laser light-scattering detector (MALLS) and an online viscometer (VS) from Wyatt Technology (Santa Barbara, CA), a differential refractive index detector (DRI) and a diode array detector (DAD) from Shimadzu (Tokyo, Japan), as described by (Buergy et al., 2020). 10 g/L of AIS were solubilized in the eluent (NaNO₃ 0.1 M with sodium azide 0.02 %) by stirring for 48 h at 4 °C, and 150 µL were injected. The ASTRA® software (Wyatt Technology, version 7.3.2.21 for PC) was used to obtain molar mass and sizes (viscometric hydrodynamic radius $\bar{R}_h(v)$) from the data as described by Buergy et al. (2020). Weight-average molar mass \bar{M}_w and intrinsic viscosity $[\eta]_w$ were obtained by integrating all the peaks. Each sample was injected twice.

3. Results

3.1. Rheological parameters of purees obtained from different cultivars/processes/contrasting nitrogen supply

All samples were shear-thinning non-Newtonian fluids and displayed weak gel behaviour as is usual for tomato products. Viscosity decreased with an increasing shear rate and the curve fitted with the Oswald de Waele model, giving access to flow behaviour indice (*n*) and consistency indice (*K*). *n* varied from 0.170 to 0.277, and (*K*) from 12.5 to 85.8 Pa s^{*n*} (Table S1). An oscillatory strain sweep confirmed that storage modulus *G'* was always higher than loss modulus *G''* under the linear viscoelastic domain, as expected for weak gels. Flow stress (FS), calculated as the point where both moduli equalised, ranged from 13 to 100 Pa, corresponding to different sample consistencies. Concerning elasticity, the phase shift (δ) ranged from 14.87 to 17.46 degrees, but it was poorly correlated to the flow stress FS ($r^2 = 0.41$) or *G'/G''* ($r^2 = 0.42$). Apparent viscosity (η_{50}) varied from 90.6 to 303.9 mPa.s (Table S1). All factors of the experimental design impacted the rheological behaviour of purees. Low nitrogen triggered a 9.3 % increase in η_{50} and a 9 % decrease in FS, while year of production had a 40 % impact on the mean η_{50} of H1311 and Terradou purees grown under unrestricted nitrogen levels. In 2020, purees had higher η_{50} , but also higher δ than in 2019. Overall, the most influential factor was the cultivar. Sailor and H1311 consistently produced purees with higher apparent viscosity than Terradou and Lycobol. Sailor had the highest η_{50} and *G'* compared even with H1311, but H1311 exhibited higher δ . The processing method was the second most influential factor: all HB purees exhibited higher η_{50} (+40 %), FS, *G'/G''* and δ than did CB purees, whatever the cultivar or year.

A PCA of all rheological parameters showed that most were strongly

correlated, along the first axis (76 % of variability). Purees were mainly differentiated by FS, *G'*, *G''*, *K* and η_{50} . The second axis (15 % of variability), related mainly to *n* and δ (Fig. 1A). Samples were differentiated on this plane by variety and process. Regarding variety, Terradou and Lycobol values were grouped together in a position corresponding to low values for most parameters, while H1311 and Sailor were located on the positive part of this axis. With regard to processing method, CB purees produced lower coordinates than HB purees on this first axis, as illustrated by the barycentre for each HB/CB group (Fig. 1B). However, processing variations behaved differently along the second axis depending on the cultivar. The variation of Terradou, Sailor and Lycobol purees involved a rightward and upward shift that corresponded to their processing method, while H1311 purees exhibited a downward shift when processed using the HB method compared to the CB method. The PCA confirmed that cultivar and processing impacts on texture cannot be distinguished by a single specific rheological behaviour, since both affect the same parameters.

3.2. Sensorial analysis discriminates between the impacts of processing method and variety

The samples which differed for their rheology where also perceived as differing by sensorial analysis (Fig. 2). In 2019, the panels distinguished the H1311 purees from the Terradou purees along the first average mapping axis and the HB/CB purees along a second axis. The impact of processing method was more strongly perceived for H1311 than for Terradou, as indicated by the greater Euclidian distances between average points on the map. No distinction was made between purees derived from tomatoes cultivated under LN and HN (Fig. 2A). In 2020, the CB and HB processes were distinguished for each of the four varieties tested, but varieties presented overlapping ellipses. Nevertheless, Terradou and H1311 purees were still fully distinguished (Fig. 2B). The most strongly contrasted varieties according to both the rheology of their purees and sensorial analysis were H1311 and Terradou.

3.3. Links between variations in puree viscosity and structural and biochemical parameters

Eleven biochemical and structural variables potentially related to texture exhibited variations according to cultivar, break process and year but were less influenced by nitrogen supply (Table 1). Each variable was individually tested for its correlation to variations in η_{50} . The variables related to the pulp fraction (AIS, proportion of large particles, pulp DMC and pulp volume fraction) had correlation coefficients higher than 0.5, but none of their individual variations fully explained the variation in viscosity. Coefficients varied between < 0,001 and 0.84, and the low correlation coefficient cannot be explained by non-linear regression between variables (data not shown). None of the variables was correlated to variations in DMC or Brix for fresh fruit, confirming that the differences observed in purees cannot be explained by a difference in the concentration steps of the process. This was confirmed by the low correlation coefficient between η_{50} and puree DMC (0.45), indicating that DMC was not an indicator of puree viscosity in our trial. In the case of serum, H1311 and Terradou displayed similar serum DMCs, but contrasting serum viscosities (η_{100}) indicating that, here, composition drives viscosity. Interestingly, serum η_{100} results were poorly correlated to those of puree η_{50} , suggesting that serum alone may not change viscosity, but may do so in association with other puree constituents.

We therefore first calculated a partial least square (PLS) model including all the variables to check if these were correlated to viscosity when combined. The PLS approach was chosen due to the colinearity observed between some variables. It was possible to calculate a significant model ($R^2 = 0.86$) involving seven out of the 11 variables (VIP > 0.8), confirming that most of our markers have a partial impact on viscosity and suggesting that they are worth considering in combination

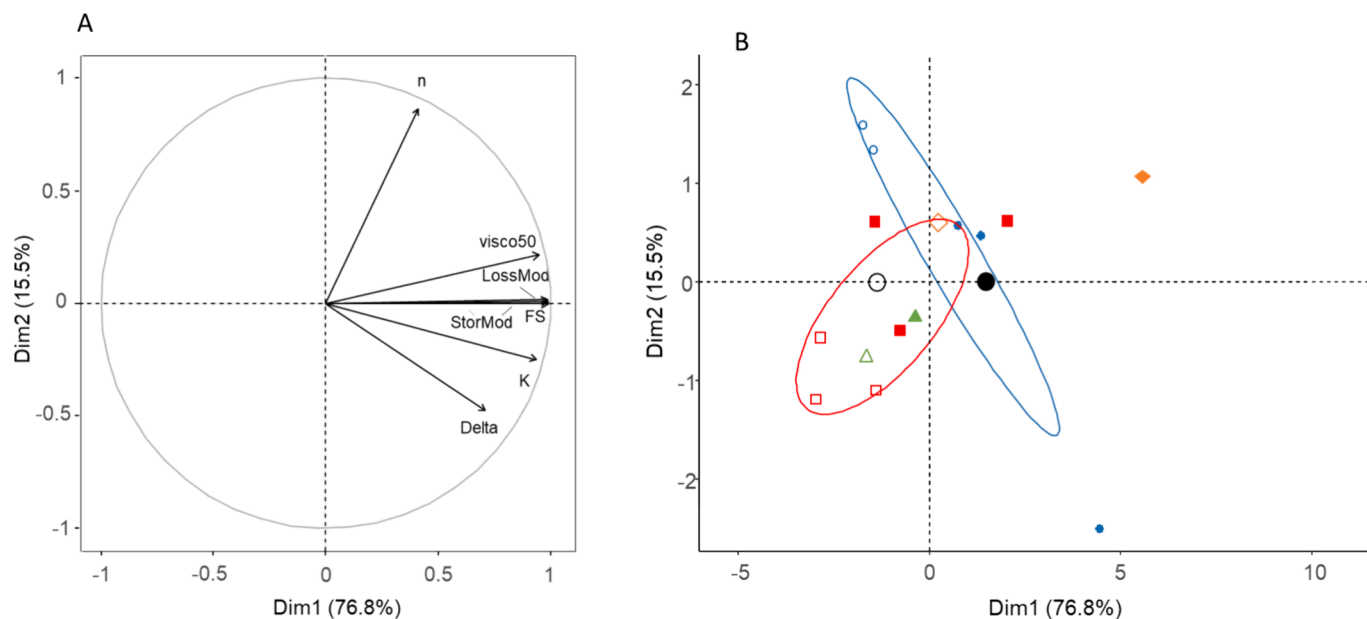


Fig. 1. Principal Component Analysis of rheological parameters for tomato purees obtained from different cultivars, nitrogen fertilization levels and processes. Circle of correlations (A) and individuals graph (B). Each point represents one puree (16 in total). Shapes and colors designate cultivars: blue circles = H1311; red squares = Terradou; green triangles = Lykobil; orange diamonds = Sailor. Unfilled symbols = CB method and solid symbols = HB method. Solid and unfilled circles are barycenters of CB and HB purees. Confidence ellipses at 95 % are shown for H1311 (blue) and Terradou (red) samples obtained over two years.

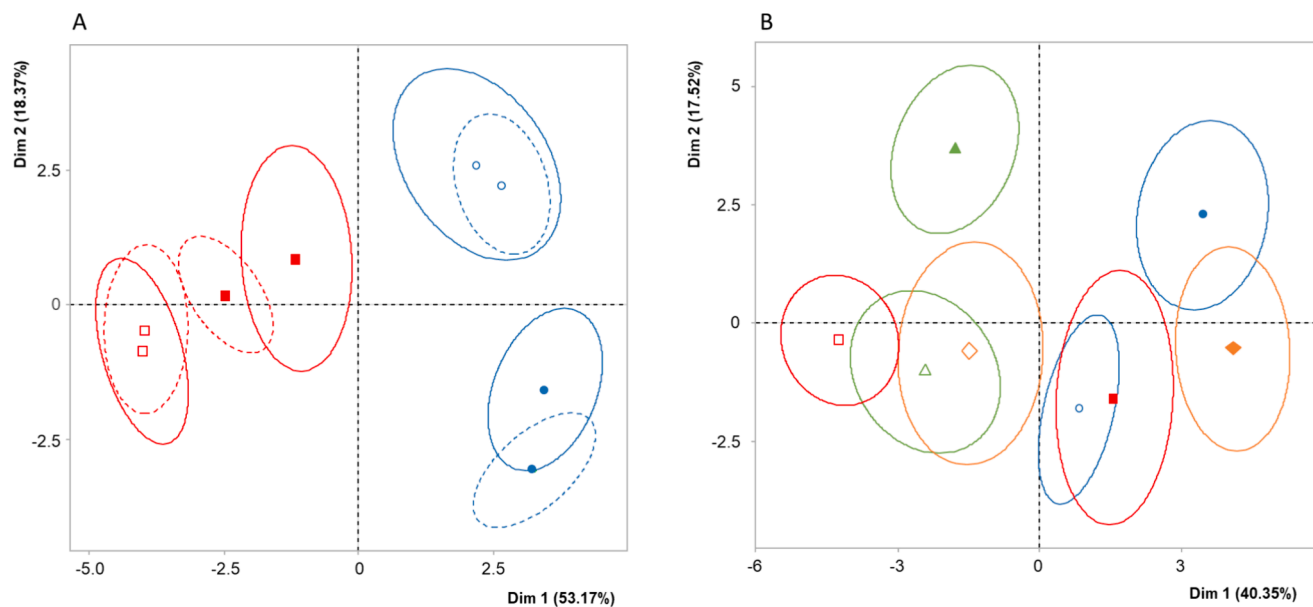


Fig. 2. Average napping patterns for purees tasted in 2019 (A) and in 2020 (B). Shapes and colors represent cultivars: blue circles = H1311; red squares = Terradou; green triangles = Lykobil; orange diamonds = Sailor. Unfilled symbols = CB method and solid symbols = HB method. Ellipses represent the sample position for 100 virtual panels generated by the bootstrap method, with 95 % confidence. Solid lines indicate HN samples and dotted lines indicate LN.

(Table S2).

We secondly performed two PLS discriminant analyses (PLS-DA) on the 12 purees from the H1311 and Terradou varieties present in 2019 and 2020. No significant models were found to differentiate between the years or nitrogen levels. However, it was possible to calculate one significant model that could discriminate between purees by either break process or variety (Table S2). The order of importance of the variables (VIP) changed from one causal factor to the other. To discriminate between CB and HB purees, AIS quantity, serum viscosity and proportion of large particles were the major variables, whereas the distinction between Terradou and H1311 mainly depended on pulp volume, overall

DMC and serum DMC (Table S2).

3.4. Composition of alcohol insoluble solids and conformation of soluble pectins

Since AIS quantity and serum viscosity emerged as key variables in PLS-DA to discriminate between processes, the purees' composition and soluble pectin conformation were studied in further detail. The major components of the AIS were GalA and glucose, confirming that they were mainly composed of pectin and cellulose. Xylose also confirmed the presence of hemicellulose. H1311 fresh fruits contained 29.8 % more

Table 1

Table of biochemical and structural variables evaluated in tomato purees processed in a pilot plant in 2019 and 2020. HN = High Nitrogen fertilization in the field, LN = Low Nitrogen fertilization in the field. CB and HB are respectively Cold Break and Hot Break processes.

| | η_{50} | Serum DMC | DMC | TSS | TA | pH | AIS | Proportion of small particles | Proportion of large particles | Pulp volume fraction | Pulp DMC fraction | Serum η_{100} |
|---------------------------------------|-------------|-------------|--------------|-------------|--------------|-------------|---------------|-------------------------------|-------------------------------|----------------------|-------------------|--------------------|
| | (mPa s) | (g/100 g) | (g/100 g) | (°Brix) | (mEq/100 g) | | (g/100 g DMC) | (% of puree DMC) | (% of puree DMC) | (% of puree volume) | (% of puree DMC) | (mPa s) |
| 2019 | 1326 | 15.0 | 15.7 | 15.1 | 14.5 | 4.4 | 17.4 | 5.1 | 16.8 | 25.4 | 33.6 | 1.8 |
| 2020 | 1990 | 14.8 | 16.7 | 15.9 | 15.5 | 4.3 | 18.6 | 3.5 | 19.4 | 25.7 | 36.8 | 2.0 |
| HN | 1747 | 14.9 | 16.4 | 15.6 | 15.2 | 4.3 | 18.4 | 4.1 | 18.5 | 25.7 | 35.8 | 1.9 |
| LN | 1391 | 15.1 | 15.7 | 15.2 | 14.3 | 4.4 | 16.7 | 5.1 | 16.9 | 24.9 | 33.2 | 1.8 |
| CB | 1232 | 15.3 | 15.9 | 15.9 | 15.2 | 4.4 | 15.7 | 4.8 | 15.8 | 25.3 | 32.6 | 1.7 |
| HB | 2085 | 14.6 | 16.4 | 15.1 | 14.9 | 4.3 | 20.3 | 3.9 | 20.4 | 25.8 | 37.7 | 2.1 |
| H1311 | 1890 | 14.2 | 15.7 | 14.8 | 15.7 | 4.3 | 19.8 | 5.0 | 19.5 | 28.0 | 38.9 | 1.8 |
| Lycobol | 1287 | 14.7 | 16.1 | 15.3 | 14.0 | 4.3 | 16.3 | 4.8 | 18.2 | 24.0 | 34.7 | 1.8 |
| Sailor | 2686 | 15.0 | 17.3 | 16.4 | 15.2 | 4.4 | 20.9 | 3.0 | 21.6 | 28.7 | 39.6 | 1.9 |
| Terradou | 1208 | 15.7 | 16.4 | 16.0 | 14.5 | 4.4 | 15.8 | 4.0 | 15.5 | 22.5 | 30.2 | 2.0 |
| Corr.to η_{50} | | 0.45 | -0.17 | 0.35 | -0.38 | 0.84 | -0.60 | 0.83 | 0.54 | 0.80 | 0.30 | -0.58 |

AIS in their DMC than Terradou fruits, on average. The H1311 AIS contained pectins that were more linear (ratio R1), less branched (R2) and with smaller branching chains (R3) compared to the Terradou AIS, but exhibiting no differences for their composition (ratio R4). The pectins in H1311 were also less methylated, which fits with the higher PME activity recorded in this variety. Mean PG activity was also higher, although the difference was affected by the year of harvest (Table S3).

The HB and CB processes decreased AIS yields by 25 % and 42 % respectively as expected given that CB treatment promotes intrinsic enzymatic action. Likewise, DM in CB puree decreases by 90 % compared to fresh fruit, while the decrease for HB puree is only 43 %, on average. The appearance of CB pectins is less linear (smaller R3) and more branched (smaller R1) compared to HB pectins, which is also consistent with a more intense PG activity in CB. Considering variety, puree AIS yields followed the differences observed in fresh fruit (higher yield for H1311 purees). However, the impacts of processing were not strictly the same for the different varieties: whereas R1 and R3 decreased from fresh to processed samples of H1311, they rose for Terradou HB samples and decreased only slightly for CB samples (Table S4).

AIS, molar mass (\bar{M}_w) and size distribution of soluble pectins differed between H1311 and Terradou purees. Soluble pectins were divided into five size classes (Fig. 3 A, B). Peaks 1, 2 and 3 were higher for H1311 pectins than for Terradou, indicating a higher proportion of high-molar-mass pectins. For both varieties, fewer pectins with hydrodynamic radius $R_h > 37.5$ nm (peak 1) were found following CB processing. Plotting molar mass vs intrinsic viscosity (Mark-Houwink plot) showed that, for high molar masses, intrinsic viscosity was higher for HB pectins (Fig. 3 C). The corresponding Mark-Houwink conformation exponent (α) was around 0.55 for CB pectins, corresponding to a random coil conformation in a θ solvent, and around 0.95 for HB, indicating a semi-flexible organization (Fishman et al., 2001). \bar{M}_w was thus higher for HB processing (1.26×10^5 g/mol) than for CB (1.01×10^5 g/mol), especially in H1311 (Fig. 3 D). The HB soluble pectins thus exhibit a more elongated structure in solution and greater \bar{M}_w , contributing to the increase of serum viscosity (Fig. 3 D) and possibly favouring interactions with the pulp fraction.

3.5. Particle size distribution and microscopic observation of structure by cultivar and processing method

In light of the PLS-DA results on the influence of particle sizes/pulp volume fraction, a detailed investigation of particle size and distribution was also conducted to ascertain differences between Terradou/H1311 and HB/CB. The insoluble content of purees had previously been divided into large (LP) and small particles (SP) as described in (Page et al.,

2019). Each fraction was first characterised for its particle-size distribution. The most contrasted fraction was the SP (Fig. 4 A and B) while LP exhibited homogeneous and monomodal profiles regardless the genotype or the process (Fig. 4 C and D). All profiles were bimodal, irrespective of variety or processing method, mainly comprising one peak between 70 and 91 μm (corresponding to the sieve mesh) and another between 5 and 20 μm . Mean size varied according to break process and variety. In the case of CB, the second peak occurred at 8 to 10 μm for both varieties, and only the respective sizes of the two peaks differed between varieties. For HB purees, the second peak differed between varieties. It occurred around 6 μm in H1311 and was the main peak. For Terradou, the second peak occurred around 15 μm , and was almost indistinguishable from the first peak. Large Particles (LP) had a monomodal distribution with a shoulder at around 50 μm . Particles were larger for Terradou (417 μm) than for H1311 (316 μm).

To study the changing size distribution of SP, a total of 103 microscopy images with double coloration targeting cell walls and lycopene were analyzed for SP prepared from each sample. A total of 614 particles were counted (328 particles of lycopene under FITC and 286 particles of cell wall material using DAPI). Particle size varied from 20 μm to 726 μm , and revealed various types of structures (Fig. 5). Merging FITC and DAPI images revealed the collocation of lycopene and cell wall fragments. Lycopene appeared either in the form of independent structures (Fig. 5A, photos a & b) or as diffuse particles forming part of an intricate structure of small fragments of cell wall (photo c). We sorted the 286 particles of cell walls into 4 categories and counted their respective frequency (Fig. 5B). A larger proportion of clusters of cell-wall material was observed in Terradou compared to H1311, especially clusters collocated with lycopene. CB treatment drastically reduced the occurrence of cell wall clusters compared to other types of particles, especially that of clusters exhibiting collocation with lycopene. Overall, the microscopy images reveal that small particles may aggregate to form complex structures larger than the sieve openings (80 μm), and this tendency to aggregate appears to be affected by processing method and variety.

4. Discussion

Variations in rheological properties induced by growing conditions, genotype and break process

Our first objective was to investigate whether there were specific rheological characteristics that depended on the particular source of variations in consistency. Genetics, growing conditions and processing methods have previously been described as having an overall impact on consistency. The originality of our study lies the combination of an

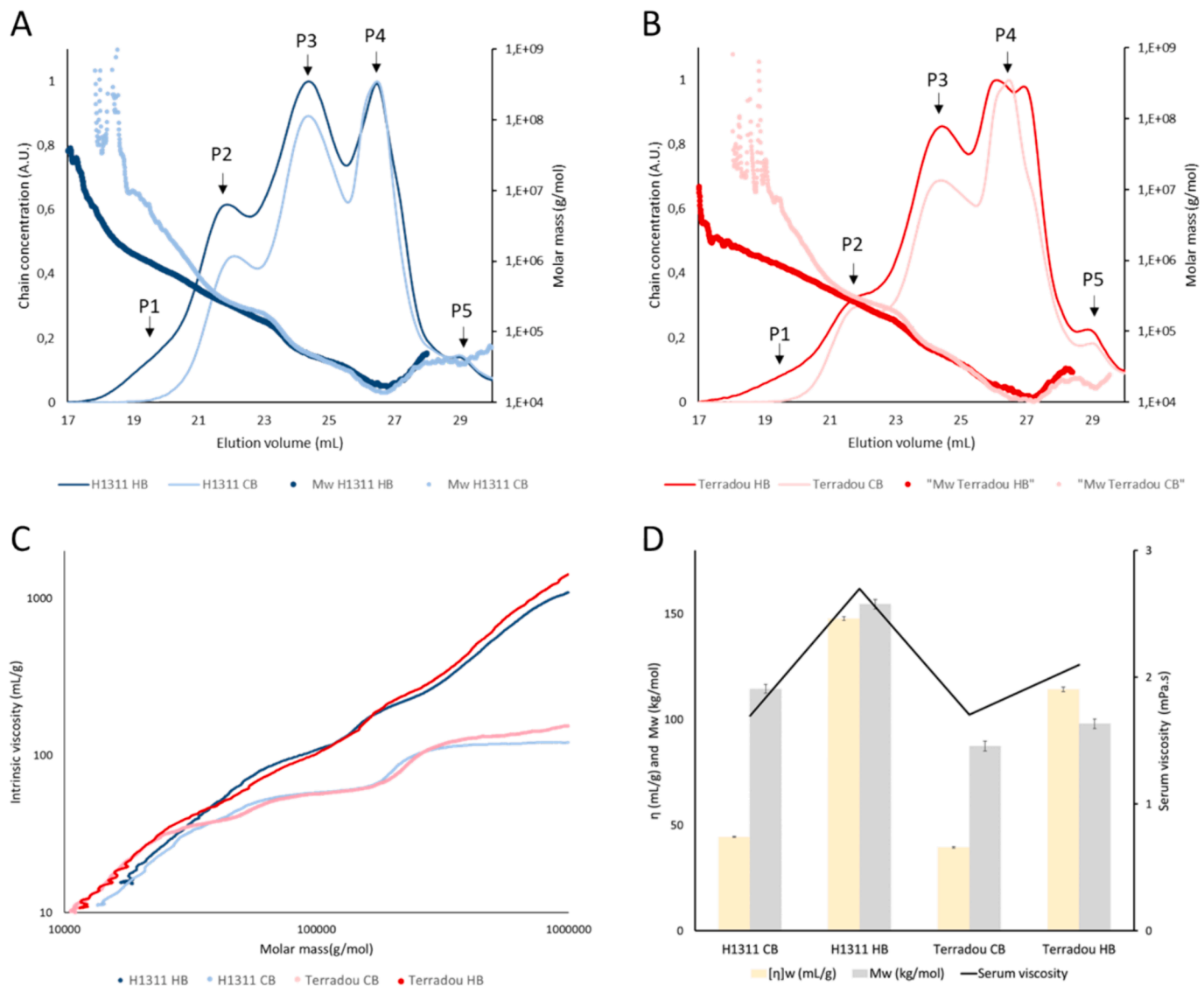


Fig. 3. Soluble pectin characteristics evaluated by HPSEC-MALLS-VS. Normalized chain concentration (thin lines) and molar mass (thick lines) versus elution volume of soluble pectins for H1311 (A) and Terradou (B), purees. Intrinsic viscosity plot versus molar mass (C) and evolution of weight-average molar mass \bar{M}_w and intrinsic viscosity $[\eta]_w$ of soluble pectins and serum viscosity for H1311 and Terradou purees (D). α : hydrodynamic coefficient for a given polymer calculated from the Mark-Houwink equation ($[\eta]_i = K_a M_i^\alpha$) for pectin samples in a 0.1 M citrate/phosphate buffer at pH 3.8. $\alpha = 0$: Spheres, 0.5–0.8: Random coils, 1.0: Stiff coils, 2.0: Rods. $\alpha = 0.913$ for H1311 HB, $\alpha = 0.551$ for H1311 CB, $\alpha = 0.974$ for Terradou HB, $\alpha = 0.567$ for Terradou CB. Arrows highlight peaks in chain concentration. P1: 15.1–20.3 mL: $R_h > 37.5$ nm, P2: 20.3–22.8 mL: 37.5 nm $> R_h > 13$ nm, P3: 22.8–25.4 mL: 13 nm $> R_h > 5$ nm, P4: 25.4–27.5 mL: 5 nm $> R_h > 2.5$ nm, P5: 27.5 mL–30 mL: $R_h < 2.5$ nm.

experimental design including several sources of variation with rheological measurements discriminating specific characteristics of elasticity and flow in purees. All our purees had the elastic properties of a weak gel and exhibited shear-thinning behavior in relation to flow, as is generally the case with tomato-based products (Diantom et al., 2017; Steffe, 1996). Shear-thinning fluids are typical of products containing large molecules or particles bound by weak bonds. Thus, when the shear rate increases, the molecules align and the particles slide past each other (Rao, 2014).

Although the rheology of the purees was affected by the year of production and, to a lesser extent, by nitrogen levels, varietal and processing effects caused the greatest and most consistent differences year on year. The H1311 variety always displayed a higher η_{50} than Terradou variety and, for each variety, the HB puree always had the highest η_{50} (Table 1).

However, it was not possible to identify a specific rheological response to either variety or process. Indeed, principal component

analysis of all rheological variables shows that most of them are highly correlated in our trial along the first axis, comprising 76.8 % of the variability. Whether they are related to elasticity or flow, they are modified in the same direction regardless of the cause. Only H1311 responded slightly differently to the break processes compared to Terradou, Sailor, and Lycobol, being the only variety to display differences in parameters n and δ between HB and CB purees.

Textural differences due to variety and processing method are perceived by hedonic analysis

The non-specific findings of the rheological analysis prompted us to check whether textural differences caused by variety or processing method could be discriminated through sensory analysis. Here, when untrained panelists were presented with simple dichotomies (2 contrasting varieties, 2 processes and 2 fertilisation modes in 2019) they were able to distinguish effects of variety from those of processing method but not fertilisation modes, in line with the rheological analysis. When faced with a wider selection of 4 varieties, they still perceived the

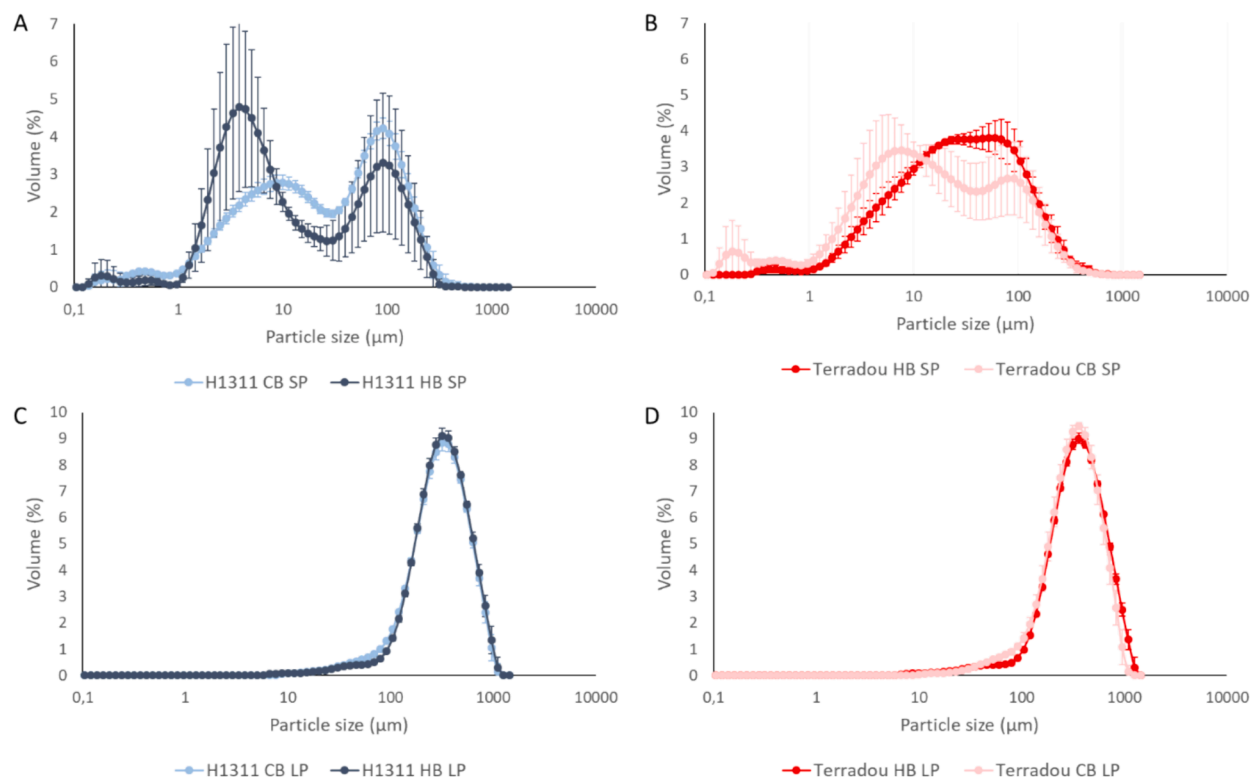


Fig. 4. Particle size distribution of Small Particles SP (A,B) and Large Particles LP (C, D) for H1311 and Terradou purees after water sieving in 2020. Distributions are the average distribution of 3 purees, each analysed twice in the granulometer, and bars indicate the standard mean error.

HB/CB difference for each variety, but did not distinguish it in the same way for each. The limitation was that texture attributes were not differentiated from other sensory criteria, therefore the rankings for each variety may have been biased by other criteria. For this reason, in the remainder of the study, the analysis included criteria influencing flavour (pH, TSS, TA) in parallel with the more physical criteria (DMC, pulp volume).

Physico-chemical origins differed according to the source of textural variations

Individually, several criteria showed a correlation with the variations in overall viscosity (η_{50}), but none was specifically related to a possible variation source (Table 1). In particular, the correlation between viscosity and dry matter content was low, allowing no discrimination between varieties or processes. This result, together with the DMC of fresh fruit, indicates that the observed differences cannot be attributed to differences in concentration intensity between samples to achieve the same TSS. PLS analysis of the variations showed, instead, that overall viscosity variations result from phenomena causing variables to combine in different ways: seven of the 11 parameters measured had a combined influence on the viscosity changes. Those influencing taste (pH, TA, TSS) had a weak influence ($VIP < 0.85$) while those influencing puree structure (proportion of large particles, proportions of pulp/serum) were in the majority.

To discriminate between break processes, the viscosity of the serum and AIS content are the main indicators, which is not surprising given that CB processing favours the action of the two main pectinolytic enzymes PME and PG, whereas HB inhibits them at a very early stage. The joint action of these two enzymes results in the depolymerisation of pectins, not only reducing the total AIS, but also the molar mass of the pectins, releasing soluble monomers which act less on viscosity. Less expected was the relative importance of the parameters related to large particle size distribution, leading us to hypothesise that changes in pectins might alter their ability to adhere to other elements, affecting particle agglomeration.

Discrimination between H1311 and Terradou varieties was most strongly dependent on pulp-related parameters (relative volume and weight), which is also in line with the different agglomerative capacities of their mash constituents. Here, though, the other important variables were serum DMC and to a lesser extent TSS ($VIP > 1$), suggesting a difference in the underlying mechanisms involved. In addition, H1311 displayed a higher AIS (constituent sugar) content and a lower TSS than Terradou, which could suggest improved agglomerative capacity due to higher pectin levels. The AIS composition of each cultivar nevertheless revealed that there is also a qualitative dimension to the differing pectin behaviours.

Pectin composition and conformation is a key factor in textural variation

Although H1311 and Terradou pectins differed in fresh fruit, processing smoothed out their differences in composition. In H1311 fresh fruit, pectins were more abundant, more linear, less branched and also slightly less methylated. But pectins in this variety appear more sensitive to the reversal of the trend that processing induces in purees: although still more abundant, pectins in H1311 purees were less linear and showed relatively more branching compared to Terradou. Soluble pectins in AIS also exhibited more high-molar-mass forms but their intrinsic viscosities were similar. Thus, the pectins of H1311 purees can be assumed to have a greater ability to generate electrostatic interactions due to their number, size and degree of branching.

With regard to the impacts of processing method, HB pectins were always more abundant and richer in galacturonic acids than CB pectins, reflecting less enzymatic degradation of linear zones in all varieties. HB purees also contain more high-molar-mass pectins than CB purees, with a higher intrinsic viscosity. The hydrodynamic coefficient suggests that HB pectins have a rather long and elongated shape whereas CB pectins would be closer to spherical in shape. HB pectins should therefore have more interaction capacity along their chains, as they would be more accessible over their entire surface. The combined effect of molar mass and intrinsic viscosity is highly correlated with serum viscosity, agreeing

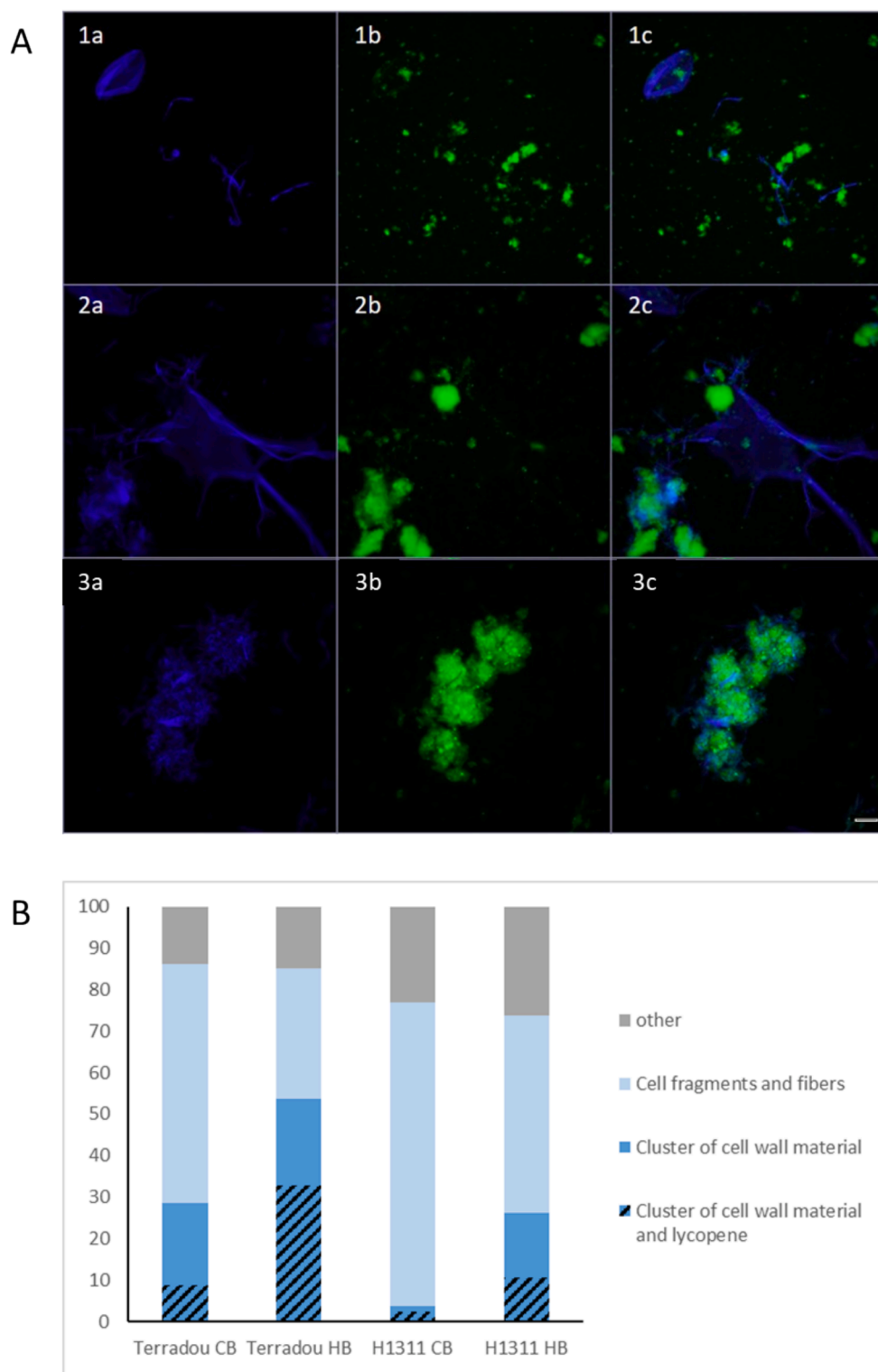


Fig. 5. (A) Typology of particles observed in CB and HB purees after sieving and (B) proportions of the different types of cell wall particles depending on variety and process. (A) Fluorescence microscope images: column a, DAPI image with cell wall material in blue marked with calcofluor, column b, FITC image with auto-fluorescent lycopene in green, column c, merged DAPI and FITC images highlighting the colocation of cell wall materials and lycopene. DAPI images show that cell wall materials were either cell fragments or fibers of differing length (1a, 2a) or a cluster of agglomerated smaller elements (3a) some of which were collocated with lycopene particles (3c). Other particles are cell ghosts (1a). FITC images show particles rich in lycopene organized either into small isolated high-density globular elements or clusters of small and more diffuse elements. The three rows show three different images representative of the range of particles observed in purees. Scale bar represents 50 μm . On the diagram (B), the portion of clusters of cell wall material collocated with lycopene is represented by black lines.

with the PLS-DA results, making this parameter very important to the discrimination of process-related effects. Last, HB puree pectins have a DM of around 12 %, while it is almost zero for CB puree. Thus, although their pectin methylation is low, HB purees pectins are likely to retain methylated areas that are more accessible due to their more linear conformation. These areas would allow interactions with more hydrophobic particles, certainly a possibility for this matrix which contains high levels of lycopene compared to other fruit.

Pectins are therefore a key component affecting the texture of tomato purees, but it seems unlikely that their intrinsic properties alone explain the differences observed. Instead, we can strongly assume that they act on the agglomerative arrangement of particles.

Processing method and variety can modify the occurrence of the collocation of lycopene and plant walls

When sieved, tomato puree dry weight falls into three main categories – soluble materials (77.6 % of DMC), particles > 80 µm forming a lightly coloured gel (18.1 % of DMC), and particles < 80 µm containing up to 80 % lycopene (4.3 %) (Page et al., 2019). The size distribution of large particles (LP) was fairly homogeneous. By contrast, the size distribution of particles < 80 µm was more variable and appears to be bimodal. Microscopic observation showed some of these particles to be formed from cell-fibre or cell residues possibly originating from pre-existing fruit tissue structures. Investigation of lycopene was more revealing. Staining revealed a diversity of object sizes and shapes, from small structures close to 1 µm to objects larger than 100 µm. Some were dense, and composed only of lycopene. They generally appeared singly or attached to the surface of cell fibres. These could be the conglomerates of dense crystals that can be observed in tomato cells (Egea et al., 2011). However, some others were up to 100 µm in size and were closely entangled with small cell fibres. These do not correspond to pre-existing fruit structures (the size of chloroplasts does not exceed 20 µm). Interestingly, they associated objects with opposite solubility. This aggregation capacity between lycopene and cell walls is strongly affected by processing method, representing up to 30 % of the objects counted for HB purees, but no more than 10 % for CB purees. It is known that the pulp and serum are more likely to separate after decantation in CB products compared with HB products. Structures combining (hydrophilic) walls with (hydrophobic) lycopene could help them to stabilise in the serum. These large structures emerge after sieving through an 80 µm sieve, indicating that they form by spontaneous aggregation in the filtrate.

5. Conclusion

Finally, there are several ways to modify the texture of tomato purees, involving both pre-harvest fruit quality and processing. Until now, the main technological lever used by the industry has been the concentration of dry matter, but our study clearly highlights that there are multiple influencing parameters, and that each source of variation (growing method/variety/break process) causes different changes in the structure of the puree. We clearly demonstrate the role of pectins and their modification by processing. We also reveal the great plasticity of insoluble particles. Last, the reassociative capacity of the particles appears to determine final texture. Their interactive capacities and, in particular, determination of the binding role of pectins and how interactions between genetics, environment and processing method cause these to vary, are promising areas for further investigation.

CRedit authorship contribution statement

Miarka Sinkora: Writing – original draft, Software, Methodology, Investigation, Formal analysis, Data curation, Conceptualization. **Anne-Laure Fanciullino:** Writing – review & editing, Validation, Supervision, Resources, Methodology, Investigation, Conceptualization. **Nadia Bertin:** Writing – review & editing, Validation, Supervision, Project administration, Methodology, Investigation, Conceptualization. **Robert**

Giovinazzo: Writing – review & editing, Visualization, Methodology, Investigation, Formal analysis, Conceptualization. **François Zuber:** Writing – review & editing, Validation, Methodology, Formal analysis, Conceptualization. **Alexandre Leca:** Writing – review & editing, Visualization, Supervision, Methodology, Investigation, Formal analysis, Conceptualization. **Agnès Rolland-Sabaté:** Writing – review & editing, Visualization, Supervision, Methodology, Investigation, Formal analysis, Conceptualization. **David Page:** Writing – review & editing, Writing – original draft, Visualization, Validation, Supervision, Resources, Project administration, Methodology, Investigation, Funding acquisition, Conceptualization.

Declaration of competing interest

The authors declare that they have no known competing financial interests or personal relationships that could have appeared to influence the work reported in this paper.

Data availability

Data will be made available on request.

Acknowledgements

HPSEC-MALLS-VS studies were supported by Platform 3A facilities, funded by the European Regional Development Fund, the French Ministry of Research, Higher Education and Innovation, the Provence Alpes Côte d'Azur region, the Departmental Council of Vaucluse and the Urban Community of Avignon. The author acknowledged Marielle Bogé, Patrice Reling (INRAE), Lucas Lanoie (SONITO) and Maxime Goussellet (CTCPA) for their technical assistance.

Funding

This work was supported by France Agrimer, under the Casdar funding program, projet “Tom’ability II”, [grant number ECEDP0919004242, 2019-2023].

Appendix A. Supplementary material

Supplementary data to this article can be found online at <https://doi.org/10.1016/j.foodres.2024.114495>.

References

- Diane, M., Barrett, D.M., Garcia, E., Wayne, J.E., 1998. Textural modification of processing tomatoes. *Crit. Rev. Food Sci. Nutr.*, 38(3):173–258. [Doi: 10.1080/10408699891274192](https://doi.org/10.1080/10408699891274192).
- Barringer, S.A., 2004. Vegetables : Tomato processing. In *Food Processing* (p. 473-490). John Wiley & Sons, Ltd. [Doi: 10.1002/9780470290118.ch29/](https://doi.org/10.1002/9780470290118.ch29/).
- Bayod, E., Månsson, P., Innings, F., Bergenstahl, B., & Tornberg, E. (2007). Low shear rheology of concentrated tomato products. Effect of particle size and time. *Food Biophysics*, 2(4), 146–157. <https://doi.org/10.1007/s11483-007-9039-2>
- Bayod, E., & Tornberg, E. (2011). Microstructure of highly concentrated tomato suspensions on homogenisation and subsequent shearing. *Food Research International*, 44(3), 755–764. <https://doi.org/10.1016/j.foodres.2011.01.005>
- BeMiller, J. N. (2018). *Carbohydrate chemistry for food scientists*. Elsevier.
- Blumenkrantz, N., & Asboe-Hansen, G. (1973). New method for quantitative determination of uronic acids. *Analytical Biochemistry*, 54(2), 484–489. [https://doi.org/10.1016/0003-2697\(73\)90377-1](https://doi.org/10.1016/0003-2697(73)90377-1)
- Buergy, A., Rolland-Sabaté, A., Leca, A., & Renard, C. M. G. C. (2020). Pectin modifications in raw fruits alter texture of plant cell dispersions. *Food Hydrocolloids*, 107, Article 105962. <https://doi.org/10.1016/j.foodhyd.2020.105962>
- Diantom, A., Curti, E., Carini, E., & Vittadini, E. (2017). Effect of added ingredients on water status and physico-chemical properties of tomato sauce. *Food Chemistry*, 236, 101–108. <https://doi.org/10.1016/j.foodchem.2017.01.160>
- Diaz, J. V., Anthon, G. E., & Barrett, D. M. (2009). Conformational changes in serum pectins during industrial tomato paste production. *Journal of Agricultural and Food Chemistry*, 57(18), 8453–8458. <https://doi.org/10.1021/jf901207w>
- Egea, I., Bian, W., Barsan, C., Jauneau, A., Pech, J.-C., Latche, A., Li, Z., & Cervin, C. (2011). Chloroplast to chromoplast transition in tomato fruit: Spectral confocal microscopy analyses of carotenoids and chlorophylls in isolated plastids and time-

- lapse recording on intact live tissue. *Annals of Botany*, 108(2), 291–297. <https://doi.org/10.1093/aob/mcr140>
- Englyst, H., Wiggins, H. S., & Cummings, J. H. (1982). Determination of the non-starch polysaccharides in plant foods by gas-liquid chromatography of constituent sugars as alditol acetates. *The Analyst*, 107(1272), 307–318. <https://doi.org/10.1039/an9820700307>
- Espinosa-Munoz, L., Renard, C., Symoneaux, R., Biau, N., & Cuvelier, G. (2013). Structural parameters that determine the rheological properties of apple puree. *Journal of Food Engineering*, 119(3), 619–626. <https://doi.org/10.1016/j.foodeng.2013.06.014>
- Fishman, M. L., Chau, H. K., Kolpak, F., & Brady, J. (2001). Solvent effects on the molecular properties of pectins. *Journal of Agricultural and Food Chemistry*, 49(9), 4494–4501. <https://doi.org/10.1021/jf0013171>
- Gawkowska, D., Cybulska, J., & Zdunek, A. (2018). Structure-related gelling of pectins and linking with other natural compounds : A review. *Polymers*, 10(7), 762. <https://doi.org/10.3390/polym10070762>
- Goodman, C. L., Fawcett, S., & Barringer, S. a. (2002). Flavor, viscosity, and color analyses of hot and cold break tomato juices. *Journal of Food Science*, 67(1), 404–408. Doi: 10.1111/j.1365-2621.2002.tb11418.x.
- Hayes, W. A., Smith, P. G., & Morris, A. E. J. (1998). The production and quality of tomato concentrates. *Critical Reviews in Food Science and Nutrition*, 38(7), 537–564. <https://doi.org/10.1080/10408699891274309>
- Hongsoongnern, P., & Chambers, E. (2008). A lexicon for texture and flavor characteristics of fresh and processed tomatoes. *Journal of Sensory Studies*, 23(5), 583–599. <https://doi.org/10.1111/j.1745-459X.2008.00174.x>
- Koocheki, A., Ghandi, A., Razavi, S. M. A., Mortazavi, S. A., & Vasiljevic, T. (2009). The rheological properties of ketchup as a function of different hydrocolloids and temperature. *International Journal of Food Science & Technology*, 44(3), 596–602. <https://doi.org/10.1111/j.1365-2621.2008.01868.x>
- Kubo, M. T. K., Rojas, M. L., Miano, A. C., & Augusto, P. E. D. (2019). Chapter 1 Rheological properties of tomato products. 1-25. Doi: 10.1039/9781788016247-00001.
- Le Bourvellec, C., Bouzerzour, K., Ginies, C., Regis, S., Plé, Y., & Renard, C. (2011). Phenolic and polysaccharidic composition of applesauce is close to that of apple flesh. *Journal of Food Composition and Analysis*, 24, 537–547. <https://doi.org/10.1016/j.jfca.2010.12.012>
- Lan, W., Renard, C. M. G. C., Jaillais, B., Leca, A., & Bureau, S. (2020). Fresh, freeze-dried or cell wall samples: Which is the most appropriate to determine chemical, structural and rheological variations during apple processing using ATR-FTIR spectroscopy? *Food Chemistry*, 330, Article 127357. <https://doi.org/10.1016/j.foodchem.2020.127357>
- Lee, Y., Bobroff, S., & Mccarthy, K. L. (2002). Rheological characterization of tomato concentrates and the effect on uniformity of processing. *Chemical Engineering Communications*, 189(3), 339–351. Doi: 10.1080/00986440212085.
- Leverrier, C., Almeida, G., Espinosa-Mu noz, L., & Cuvelier, G. (2016). Influence of particle size and concentration on rheological behaviour of reconstituted apple purees. *Food Biophysics*, 11(3), 235–247. Doi: 10.1007/s11483-016-9434-7.
- Leverrier, C., Moulin, G., Cuvelier, G., & Almeida, G. (2017). Assessment of deformability of soft plant cells by 3D imaging. *Food Structure*, 14, 95–103. <https://doi.org/10.1016/j.foostr.2017.07.002>
- Lopez-Sanchez, P., Nijssse, J., Blonk, H. C. G., Bialek, L., Schumm, S., & Langton, M. (2011). Effect of mechanical and thermal treatments on the microstructure and rheological properties of carrot, broccoli and tomato dispersions. *Journal of the Science of Food and Agriculture*, 91(2), 207–217. <https://doi.org/10.1002/jsfa.4168>
- Moelants, K. R. N., Cardinaels, R., Jolie, R. P., Verrijssen, T. A. J., Van Buggenhout, S., Van Loey, A. M., Moldenaers, P., & Hendrickx, M. E. (2014). Rheology of concentrated tomato-derived suspensions: Effects of particle characteristics. *Food and Bioprocess Technology*, 7(1), 248–264. <https://doi.org/10.1007/s11947-013-1070-3>
- Moelants, K. R. N., Jolie, R. P., Palmers, S. K. J., Cardinaels, R., Christiaens, S., Van Buggenhout, S., Van Loey, A. M., Moldenaers, P., & Hendrickx, M. E. (2013). The Effects of process-induced pectin changes on the viscosity of carrot and tomato sera. *Food and Bioprocess Technology*, 6(10), 2870–2883. <https://doi.org/10.1007/s11947-012-1004-5>
- Ouden, F. W. C., & Vliet, T. (2006). Particle size distribution in tomato concentrate and effects on rheological properties. *Journal of Food Science*, 62, 565–567. <https://doi.org/10.1111/j.1365-2621.1997.tb04431.x>
- Page, D., Labadie, C., Reling, P., Bott, R., Garcia, C., Gaillard, C., Fourmaux, B., Bernoud-Hubac, N., Goupy, P., Georgé, S., & Caris-Veyrat, C. (2019). Increased diffusivity of lycopene in hot break vs. Cold break purees may be due to bioconversion of associated phospholipids rather than differential destruction of fruit tissues or cell structures. *Food Chemistry*, 274, 500–509. <https://doi.org/10.1016/j.foodchem.2018.08.062>
- Pagès, J. (2005). Collection and analysis of perceived product inter-distances using multiple factor analysis: Application to the study of 10 white wines from the Loire Valley. *Food Quality and Preference*, 16(7), 642–649. <https://doi.org/10.1016/j.foodqual.2005.01.006>
- Pagés, J., & Husson, F. (2005). Multiple factor analysis with confidence ellipses: A methodology to study the relationships between sensory and instrumental data. *Journal of Chemometrics*, 19(3), 138–144. <https://doi.org/10.1002/cem.916>
- Porretta, S. (Ed.). (2019). *Tomato chemistry, industrial processing and product development*: Royal Society of Chemistry. Doi: 10.1039/9781788016247.
- Rao, M. A. (2014). *Rheology of fluid, semisolid, and solid foods : Principles and applications* (Third edition.). Imprint: Springer.
- Ribas-Agustí, A., Gouble, B., Bureau, S., Maingonnat, J.-F., Audergon, J.-M., & Renard, C. M. G. C. (2017). Towards the use of biochemical indicators in the raw fruit for improved texture of pasteurized apricots. *Food and Bioprocess Technology*, 10(4), 662–673. <https://doi.org/10.1007/s11947-016-1850-7>
- Ronga, D., Francia, E., Rizza, F., Badeck, F.-W., Caradonia, F., Montevicchi, G., & Pecchioni, N. (2019). Changes in yield components, morphological, physiological and fruit quality traits in processing tomato cultivated in Italy since the 1930's. *Scientia Horticulturae*, 257, Article 108726. <https://doi.org/10.1016/j.scientia.2019.108726>
- Saeman, J. F., Moore, W. E., Mitchell, R. L., & Millett, M. A. (1954). *Technique for the determination of pulp constituents by quantitative paper chromatography*. 37, 336–343.
- Sánchez, M. C., Valencia, C., Gallegos, C., Ciruelos, A., & Latorre, A. (2002). Influence of processing on the rheological properties of tomato paste. *Journal of the Science of Food and Agriculture*, 82(9), 990–997. <https://doi.org/10.1002/jsfa.1141>
- Steffe, J. F. (1996). *Rheological methods in food process engineering*. Freeman Press.
- Stokes, J. R. (2012). 'Oral' rheology. In *Food Oral Processing* (pp. 225–263). Ltd: John Wiley & Sons. <https://doi.org/10.1002/9781444360943.ch11>
- Valencia, C., Sanchez, M. C., Ciruelos, A., & Gallegos, C. (2004). Influence of tomato paste processing on the linear viscoelasticity of tomato ketchup. *Food Science and Technology International*, 10(2), 95–100. <https://doi.org/10.1177/1082013204043880>
- Vilas Boas, A. A. de C., Page, D., Giovino, R., Bertin, N., & Fanciullino, A.-L. (2017). Combined effects of irrigation regime, genotype, and harvest stage determine tomato fruit quality and aptitude for processing into puree. *Frontiers in Plant Science*, 8, 1-16. Doi: 10.3389/fpls.2017.01725.
- WPTC. (2021). *WPTC crop update as of 21 October 2021*. <https://www.wptc.to/pdf/releases/WPTC%20crop%20update%20as%20of%2021%20october%202021.pdf>
- Yoo, B., & Rao, M. a. (1994). Effect of unimodal particle size and pulp content on rheological properties of tomato puree. *Journal of Texture Studies*, 25(4), 421–436. Doi: 10.1111/j.1745-4603.1994.tb00772.x.